Temporal Analysis of Stationary Markov α-sub-Gaussian Noise

Ahmed Mahmood and Mandar Chitre
Acoustic Research Laboratory, Tropical Marine Science Institute, National University of Singapore
e-mail: {tmsahme, mandar}@nus.edu.sg

***Abstract*—In warm shallow waters, snapping shrimp noise is the dominant source of ambient noise at medium-to-high frequencies. The noise process is impulsive and exhibits memory. The latter property causes outliers to cluster together, thus resulting in *bursty impulsive* noise. When tuned to snapping shrimp data, the stationary α-sub-Gaussian noise with memory order m (αSGN(m)) model tracks the former's *temporal amplitude statistics* very well. In comparison to contemporary impulsive noise models, αSGN(m) offers a far more realistic model for snapping shrimp noise. To develop a more deeper understanding of αSGN(m), we perform an *impulsive event* analysis on its realizations. This is accomplished by initially mapping impulsive data to a point process in time. The resulting time-series is then analyzed via first-order interval and counting analysis. We compare our results with those of snapping shrimp noise and highlight the pros and cons of adopting the αSGN(m) model. Moreover, our results also offer us a reliable way to tune the order m of αSGN(m).**

I. Introduction

Ambient noise in the sea is known to vary considerably in different environments [1]. In warm shallow waters, the sea bed is typically littered with colonies of snapping shrimp. These crustaceans are known to create snaps (surges in acoustic pressure) by cavitating bubbles. Practical measurements have shown peak-to-peak levels of a single snap to be as high as 190 dB re 1μPa at 1 m from the source [2], [3]. The collective snaps create an impulsive soundscape in warm shallow waters [3], [4]. If not accounted for, snapping shrimp noise is detrimental to the performance of acoustic systems operating nearby [5]–[7]. Though it is known that snapping shrimp noise is impulsive, few studies have been devoted to understanding the dependence between its samples [3], [8], [9]. In fact, the contemporary literature typically adopts *white* impulsive noise models to design schemes that mitigate the detrimental impact of snapping shrimp noise on underwater systems [5], [10], [11]. In reality, snapping shrimp noise exhibits memory and is thus bursty as well as impulsive.

In [9], the authors observe that closely-spaced snapping shrimp noise samples exhibit *near-elliptic* distributions. This was highlighted by plotting delay scatter plots of recorded samples. Noting that the empirical amplitude distribution is characterized well by univariate heavy-tailed symmetric α-stable (SαS) distributions, [9] based the αSGN(m) model on the multivariate α-sub-Gaussian (αSG) distribution. The latter is essentially a multivariate heavy-tailed SαS distribution with the additional constraint of being elliptic as well [12]. The αSGN(m) model employs a sliding window framework and effectively constrains *any* adjacent $m+1$ samples to an αSG distribution. Moreover, the model does not allow the underlying αSG distribution to vary with time. Consequently, the αSGN(m) is a stationary Markov process. As marginal distributions of a multivariate SαS distribution are SαS as well [12], [13], the αSGN(m) model is able to characterize the empirical amplitude distribution of snapping shrimp noise, i.e., each sample is essentially an SαS random variable. However, due to its memory, it also tracks the amplitude statistics as a function of time and thus the *temporal amplitude statistics* of the noise process [9].

In this paper, we try to further our understanding of the αSGN(m) model by conducting interval and counting analysis of *impulsive events* on its samples. As a realization of αSGN(m) is a time-series, our study is essentially a temporal analysis of αSGN(m) data. Note, that this is not to be confused with the aforementioned temporal amplitude statistics of αSGN(m). While the latter highlights how amplitude statistics varies in time due to dependence between the samples, this work discards the sample values by converting αSGN(m) to a random point process in time. By doing so, each noise sample is mapped onto a binary value within $\{0, 1\}$, where 0 and 1 imply the absence and presence of an impulsive event, respectively. Subsequent temporal analysis offers insight into the arrival and counts of impulsive events on the real-number line. We compare our results with those of snapping shrimp noise and highlight the suitability of αSGN(m) in modeling the former. Moreover, we show that temporal analysis of impulsive events offers a clear way to estimate the order m from practical data. The latter is essential for tuning the model appropriately [9].

This paper is organized as follows: In Section II we briefly introduce the αSGN(m) model. This is followed by discussions on interval and counting analysis for αSGN(m) and snapping shrimp noise in Section III. The impact of dead-time filtering on the temporal statistics is investigated in Section IV. We wrap up by presenting our conclusions in Section V.

II. The αSGN(m) Model

The αSGN(m) model was initially introduced in [9] to model the near-elliptic dependency between immediately adjacent snapping shrimp noise samples. The model is based on the multivariate αSG distribution, which besides being heavy-tailed SαS, is elliptic as well [14]. Mathematically, an αSG

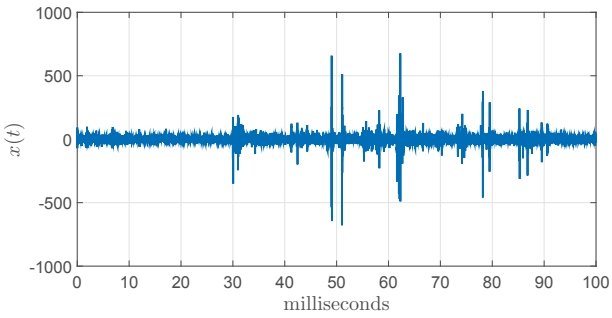

Fig. 1. A realization of snapping shrimp noise.

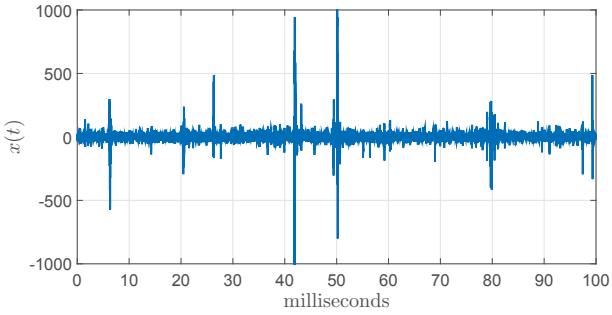

Fig. 2. A realization of αSGN(4).

random vector $\vec{X}$ is defined as

$$\vec{X} \overset{d}{=} A^{1/2}\vec{G}, \tag{1}$$

where $\overset{d}{=}$ signifies equality in distribution, A is a totally-right skewed *stable random variable* and $\vec{G}$ is a multivariate zero-mean Gaussian random vector with covariance matrix $\mathbf{R} = [r_{ij}]$, i.e., $\vec{G} \sim \mathcal{N}(\mathbf{0}, \mathbf{R})$. Both A and $\vec{G}$ are statistically independent of one another [12], [15].

The PDF of a stable random variable is completely defined by four parameters, namely, the characteristic exponent $\alpha \in (0, 2]$, skew $\beta \in [-1, 1]$, scale $\delta \in (0, +\infty)$ and location $\mu \in (-\infty, +\infty)$ [14], [15]. The distribution can be denoted succinctly by $\mathcal{S}(\alpha, \beta, \delta, \mu)$. An S$\alpha$S random variable is stable but with the additional constraint of $\beta = \mu = 0$ [14], [15]. Consequently, an SαS distribution may be represented by $\mathcal{S}(\alpha, \delta)$. Of all parameters, α completely determines the tail-heaviness of a stable distribution [14], [15]. In fact, the heaviness decreases monotonically with increasing α. Moreover, for $\alpha = 2$, the distribution ceases to depend on β and is Gaussian with mean μ and variance $2\delta^2$, i.e., $\mathcal{S}(2, \beta, \delta, \mu) \overset{d}{=} \mathcal{N}(\mu, 2\delta^2)$ [14], [15]. On a final note, we see that *all* marginal distributions of an αSG random vector are αSG (and thus SαS) as well [14]. Consequently, by setting $A \sim \mathcal{S}(\frac{\alpha}{2}, 1, 2(\cos(\frac{\pi\alpha}{4}))^{2/\alpha}, 0)$, the i^{th} univariate marginal of $\vec{X}$ in (1) is SαS distributed with $\mathcal{S}(\alpha, \sqrt{r_{ii}})$ [12].

The αSGN(m) model is based on a sliding-window framework and constrains any adjacent $m + 1$ samples to an αSG distribution [9]. Mathematically, let $X_n \ \forall \ n \in \mathbb{Z}$

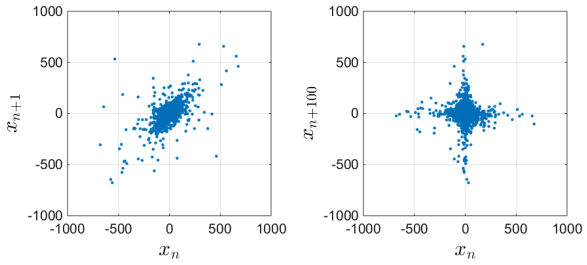

Fig. 3. Delay scatter plots of snapping shrimp noise.

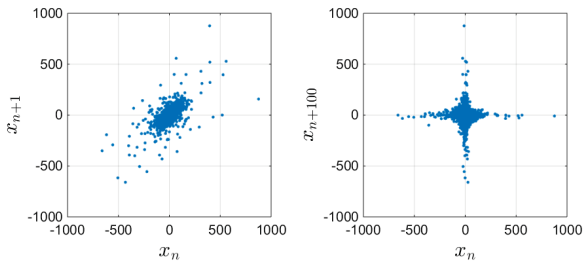

Fig. 4. Delay scatter plots of αSGN(4).

denote samples of αSGN(m) at time index n and $\vec{X}_{n,m} = [X_{n-m}, \ldots, X_{n-1}, X_n]^{\mathsf{T}}$ a random vector in $\mathbb{R}^{m+1}$ consisting of X_n and m immediately previous samples. Then, from (1), the following expression *completely* defines the process [9]:

$$\vec{X}_{n,m} \overset{d}{=} A_n^{1/2}\vec{G}_{n,m}, \tag{2}$$

where $\vec{G}_{n,m} = [G_{n-m}, \ldots, G_{n-1}, G_n]^{\mathsf{T}}$ is a multivariate zero-mean Gaussian random vector with covariance matrix $\mathbf{R}_m \in \mathbb{R}^{(m+1)\times(m+1)}$, i.e., $\vec{G}_{n,m} \sim \mathcal{N}(\mathbf{0}, \mathbf{R}_m)$ and $A_n \sim \mathcal{S}(\frac{\alpha}{2}, 1, 2(\cos(\frac{\pi\alpha}{4}))^{2/\alpha}, 0) \ \forall \ n \in \mathbb{Z}$. From (2), one notes that αSGN(m) is a Markov process of order m [9]. Moreover, as $\mathbf{R}_m$ does not vary with time, αSGN(m) is a stationary Markov process. The sliding-window framework and stationarity of the process also ensure that $\mathbf{R}_m = [r_{ij}]$ is a *symmetric Toeplitz matrix* [9]. Consequently, it takes on the block form

$$\mathbf{R}_m = \begin{bmatrix} \mathbf{R}_{m-1} & \mathbf{r}_m \\ \mathbf{r}_m^{\mathsf{T}} & r_{(m+1)(m+1)} \end{bmatrix}, \tag{3}$$

where $\mathbf{r}_m = [r_{1(m+1)}, r_{2(m+1)}, \ldots, r_{m(m+1)}]^{\mathsf{T}}$. Due to its structure, $\mathbf{R}_m$ can be *completely* constructed from a single row or column. Further still, its main diagonal elements are equivalent. Therefore, by setting $r_{ii} = \delta^2 \ \forall \ i \in \{1, 2, \ldots, m+1\}$, we note that $X_n \sim \mathcal{S}(\alpha, \delta) \ \forall \ n \in \mathbb{Z}$.

We plot a realization $x(t)$ of snapping shrimp noise (sampled at 180kHz) in Fig. 1 and of αSGN(4) in Fig. 2. The latter's parameters are *tuned* to that of the snapping shrimp noise dataset via the methodology outlined in [9]. One can see the similarities between both realizations. Moreover, denoting the samples as x_n, we present delay scatter plots of either realization in Figs. 3 & 4, respectively. The scatter plots are generated for delays of 1 and 100. For snapping shrimp noise, one can clearly see an elliptic geometry associated with the

TABLE I
$\hat{r}_{1k}$ TUNED TO SNAPPING SHRIMP NOISE.

k	$\frac{\hat{r}_{1k}}{\hat{\delta}^2}$
1	1.000
2	0.687
3	0.342
4	0.202
5	0.066
6	0.045
7	0.024
8	-0.034
9	-0.096

scatter plot in Fig. 3. With increasing delay, the samples are expected to be decreasingly dependent. When the delay is large enough, the samples are effectively independent and the scatter plot converges to a four-tailed structure akin to that observed at a delay of 100 in Fig. 3 [7]. From visual judgment, on comparing Figs. 3 & 4, we clearly see that the tuned αSGN(4) model characterizes the temporal amplitude statistics of snapping shrimp noise sampled at 180 kHz very well. We analyze temporal statistics of impulsive events for both processes next.

III. Temporal Analysis of αSGN(m) and Snapping Shrimp Noise

Though αSGN(m) effectively models the temporal amplitude statistics of the snapping shrimp noise process, the temporal characteristics of its impulsive events are yet to be understood. This can be accomplished by doing away with the sample values and modeling αSGN(m) as a *random point process*. The latter is roughly defined as a collection of highly localized events or random points that occur in some space [16]. For the case of snapping shrimp noise, related numerical studies were carried out in [3], [8], [17] and a number of observations were made. The primary objective of this paper is to model αSGN(m) as a point process in time and compare its results to those observed in snapping shrimp noise. Moreover, we conduct a similar analysis on white SαS noise (WSαSN). The latter essentially is an αSGN(0) process, i.e., it has no memory and its samples are IID SαS random variables [9]. The WSαSN model has been used extensively in the literature to model the amplitude distribution of snapping shrimp noise but fails to address the burstiness associated with the noise process [9].

A. Data Setup & Processing

To allow fair comparison, we tune the parameters of the αSGN(m) model to empirical snapping shrimp data. In our work, we consider an 1800 s recording of snapping shrimp noise sampled at 180 kHz. The data was recorded in Singapore waters by personnel of the Acoustic Research Laboratory at the National University of Singapore. We divide the dataset into blocks of 10^6 samples (~ 5.56 s) and estimate the model's parameters for each block for a *maximum predetermined* order of $m = 8$ using the method outlined in [9]. More precisely, for each block, α and δ are evaluated via maximum-likelihood estimation. These are then used to get the remaining elements of $\mathbf{R}_8$ via a covariation based method [9], [18]. The final values of α, δ and $\mathbf{R}_8$ are acquired by averaging the corresponding estimates over all blocks. These estimated values (with obvious notation) are $\hat{\alpha} = 1.57$, $\hat{\delta} = 14.63$ and $\hat{r}_{1k}\ \forall\ k \in \{1, 2, \ldots, 9\}$ in Table I. We have listed only the first row of the *normalized* covariance matrix $\hat{\mathbf{R}}_8/\delta^2$ in Table I, as $\hat{\mathbf{R}}_8$ can be completely constructed from it. Finally, we note that the employed estimation method for α and δ is independent of m [9]. Moreover, from (3), $\mathbf{R}_m$ for $m < 8$ is essentially the $(m+1) \times (m+1)$ top-left block matrix of $\mathbf{R}_8$. Therefore, by estimating parameters for αSGN(8), we already have estimates of the model's parameters for $m < 8$.

To accomplish our goals, we need to employ a suitable *event detector* to convert αSGN(m) realizations to that of a point process [3], [8]. From Fig. 2, one can intuitively see that an impulsive event can be adequately detected if the amplitude of a noise sample is observed to exceed a suitable threshold. In our work we employ a *threshold detector* with threshold $20\hat{\delta}$. A sample outcome $X_n = x_n$ is mapped on to 0 or 1 if $x_n < 20\hat{\delta}$ or $x_n \geq 20\hat{\delta}$, respectively. Mathematically,

$$p_n = \begin{cases} 1 & \text{if } x_n \geq 20\hat{\delta} \\ 0 & \text{otherwise} \end{cases}, \tag{4}$$

where p_n is the observation of the point process at index n. Note that we do not define a *negative* impulse, i.e., $x_n \leq -20\hat{\delta}$, as an impulsive event. This is due to the fact that negative surges in pressure for snapping shrimp noise are attributed to surface reflections of snaps [3]. Nevertheless, there is no loss in generality as considering negative snaps just increases the number of impulsive arrivals by a factor of two. The latter stems from the fact that an αSGN(m) sample has a zero-centered symmetric PDF, i.e., $X_n \sim \mathcal{S}(\alpha, \delta)$.

Event analysis techniques can be broadly divided into two different categories, namely, interval and counting analysis [3]. In either case, the point process data is divided into blocks before processing. The former characterizes time delay (or number of samples) between ordered events, while the latter counts the number of events in a certain time block. Both approaches are covered in our work. For the first case, we employ an inter-event interval (II) technique which counts the time delay T_D between immediately adjacent (first-order) events and computes an empirical PDF. When plotted on a log scale, the resulting curve is *linear* if it is an *exponential* distribution [3], [8]. This in turn shows that the point process belongs to the general Poisson family. Secondly, for counting analysis, we compute the Fano-factor (FF) time curves. These are evaluated from the *variance* to *mean* ratio of the time samples and are plotted against the time duration T_N of the employed block [3], [8]. If the point process is homogeneous Poisson, the FF plot is a straight line of amplitude one.

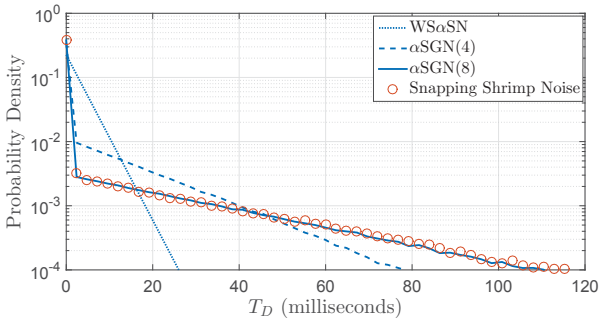

Fig. 5. PDFs of first-order inter-event intervals.

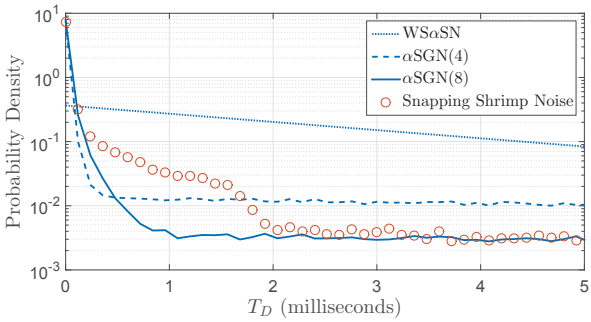

Fig. 7. PDFs of first-order inter-event intervals (near origin).

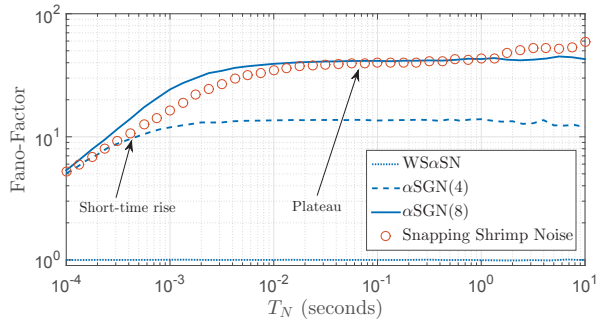

Fig. 6. Fano-factor against block length.

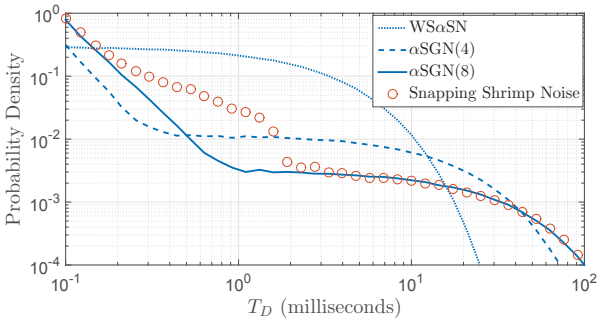

Fig. 8. PDFs of first-order inter-event intervals on a log-log scale.

B. Results and Discussion

In the literature, II and FF analysis for snapping shrimp noise have clearly shown the latter *not* to be a homogeneous Poisson process [3], [8]. We highlight this by presenting II results in Fig. 5. The red markers highlight the empirical PDF of first-order IIs plotted against T_D (measured in milliseconds) of the snapping shrimp noise dataset, while the blue curves correspond to αSGN(m) for $m \in \{0, 4, 8\}$. Note that the curve corresponding to WSαSN is essentially that of a homogeneous Poisson process as its samples are IID random variables. We also note that the remaining curves become linear as T_D increases. This is because the first-order II probability density at T_D is conditional on observing an event at $T_D = 0$ ms and none in between. With increasing T_D, the PDF ceases to be influenced by events located far in the past and depends on nearby samples only, which in turn *do not* observe impulsive events. Therefore, for *large* T_D, event arrivals are independent of that at $T_D = 0$ ms and can be approximated by an exponential distribution. This results in the linear regions when plotted on a log-scaled axis.

Fig. 5 offers us great insight into how m influences the effectiveness of the αSGN(m) model. Clearly, in our case, αSGN(8) adequately models inter-arrival events for the considered snapping shrimp noise data set. Moreover, as expected, WSαSN is ineffective in modeling memory and thus the intervals between adjacent snaps. The PDF corresponding to αSGN(4) offers a better fit than that of WSαSN, but offers a higher rate of impulsive events (lower gradient) with respect to the snapping shrimp case. These results are also supported by their corresponding FF plots presented in Fig. 6. Following [17], the latter are plotted on a log-log scale against T_N (measured in seconds). As samples of WSαSN are IID random variables, its FF curve is flat. Clearly, this deviates sharply from the FF plot of snapping shrimp noise. In comparison, the αSGN(8) curve tracks the latter much more effectively. The *short-time rise* and *plateau* regions in Fig. 6 arise mainly due to surface reflections of a snapping shrimp snap [3], [8]. We note the αSGN(8) curve approximates the plateau region $10^{-2} < T_N \leq 10^{0}$ (seconds) of its snapping shrimp counterpart very well. However, it also deviates in the short-time rise region $10^{-4} < T_N \leq 10^{-2}$ (seconds). Moreover, we also observe a slight deviation between the curves for $T_N > 10^{0}$ s. The latter is due to the non-stationarity of ambient noise in warm shallow waters, which mainly includes snapping shrimp noise but also other biological/man-made noise as well.

In Fig. 5, on closer inspection, we note that the snapping shrimp noise and αSGN(m) curves for $m \neq 0$ sharply decrease near the origin. It is insightful to see how they vary when T_D is small. To highlight this we plot the same II curves, but for $T_D \in [0, 5]$ ms in Fig. 7. Though αSGN(8) clearly tracks the rate of impulsive arrivals in the snapping shrimp noise dataset for large T_D (observed in Fig. 5), it does not exhibit the same II characteristics for $0.2 < T_D \leq 2$ (milliseconds) in Fig. 7. This may be because the considered dataset also consists of samples from other sources of noise with lingering dependencies. We also note, that for $T_D \sim 0$ ms,

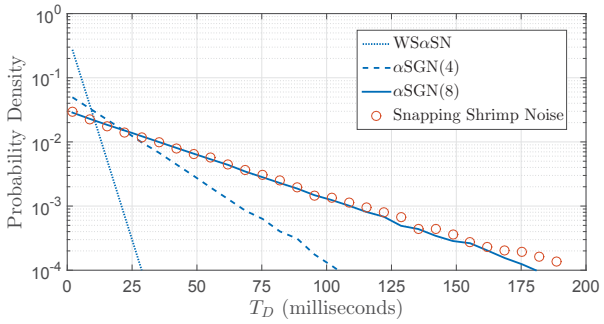

Fig. 9. PDFs of first-order inter-event intervals with dead-time filtering.

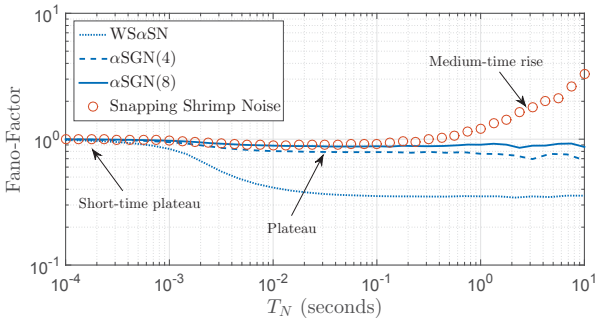

Fig. 11. Fano-factor against block length with dead-time filtering.

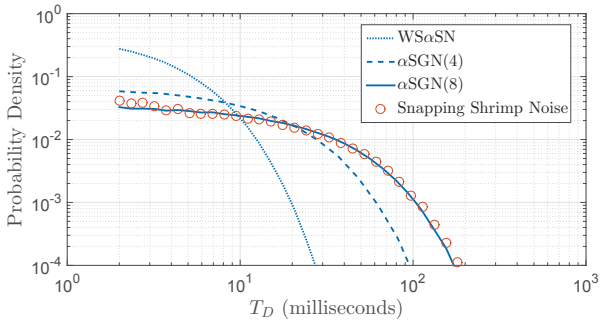

Fig. 10. PDFs of first-order inter-event intervals with dead-time filtering on a log-log scale.

both αSGN(4) and αSGN(8) offer good approximates to the snapping shrimp curve. This is expected as both models share similar parameter estimates ($\hat{\mathbf{R}}_8$ consists of $\hat{\mathbf{R}}_4$) and they are designed to characterize $m+1$ immediately adjacent samples. Finally, to highlight II characteristics for both small and large T_D, we also present the II results on the log-log scale in Fig. 8. The latter we believe, is a better visualization than traditional log-scale plots such as those in Figs. 5 & 7.

On a final note, we observe that the II plots in Figs. 5 & 8 offer us a way to select m for αSGN(m) when it comes to modeling snapping shrimp noise. In our case, $m = 8$ offers the best fit. As highlighted by Figs. 1 - 4, the *temporal amplitude statistics* may erroneously lead us in selecting m other than what actually might be. The II curves on the other hand clearly differentiates between αSGN(m) for varying m and thus offer us a very clear method of choosing m.

IV. Temporal Analysis with Dead-Time Filtering

Till now we have investigated impulsive events in αSGN(m) tuned to snapping shrimp noise and compared it to the latter. However, we note that a burst in αSGN(m) effectively models the collective response of *two* different phenomenon originating from a *single* snapping shrimp snap. The first is the temporal response of the snap and the second is the multipath component due to surface reflection [3], [8]. Therefore, a burst arises from a single snap. Section III offers useful insights in to scenarios involving signal transmission in warm shallow waters. In such settings, receivers need to ideally compensate for noise bursts that accompany the signal. Therefore, temporal characteristics within *small* ranges of T_D and T_N are of interest. In underwater acoustic communication, this typically amounts to sub-millisecond values.

In the literature, various works on snapping shrimp noise also define an impulsive event as individual snap arrivals, i.e., a burst is counted as a single event [3], [8]. This is useful in scenarios where one is interested in determining the position/density of snapping shrimp populaces or mapping objects within the vicinity of such a populace. Thus, to avoid counting clustered impulses as different events, further processing of p_n is necessary before employing II and FF analysis. Following [3], [8], we investigate the temporal characteristics of our data with *dead-time filtering*. The latter is easily implemented and does not search for potential events within a certain interval of a detected impulse [3]. We define our dead-time filter to negate all impulsive events within $T_D < 2$ ms. The motivation for this arises from Figs. 7 & 8, where one can clearly see the snapping shrimp curve at the end of its clustering phase.

In Figs. 9 & 10, we present first-order II PDFs for snapping shrimp and αSGN(m) realizations on log and log-log scales, respectively. As expected, our setting of the dead-time zone to 2 ms effectively nullifies dependence of impulsive events (for $T_D \geq 2$ ms) on the event observed at $T_D = 0$ ms. This results in linear curves in Fig. 9 which are similar to what one observes for homogeneous Poisson data with dead-time filtering [3]. The corresponding FF curves presented in Fig. 11 exhibit some interesting properties. Introducing dead-time filtering essentially regularizes the data for $T_N \ll 2$ ms, which results in it behaving like a homogeneous Poisson process, i.e., FF ~ 1 as $T_N \to 0$ ms [3]. On comparison with Fig. 6, we see that the short-time rise is non-existent and is re-labeled in Fig. 11 as a *short-time plateau*. The αSGN(8) process is able to track this and the *plateau* region very well. More significant though is the deviation observed at $T_N \sim 0.3$ s, labeled as *medium-time rise*. This is attributed to the non-stationarity of the snapping shrimp noise data set and is not as pronounced in Fig. 6.

As a final result, we investigate the impact of changing the threshold in (4) to $30\hat{\delta}$ in addition to dead-time filtering. Increasing the threshold reduces the number of impulsive

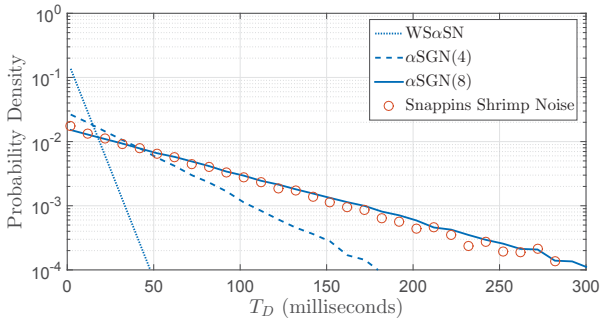

Fig. 12. PDFs of first-order inter-event intervals with dead-time filtering and threshold $30\hat{\delta}$.

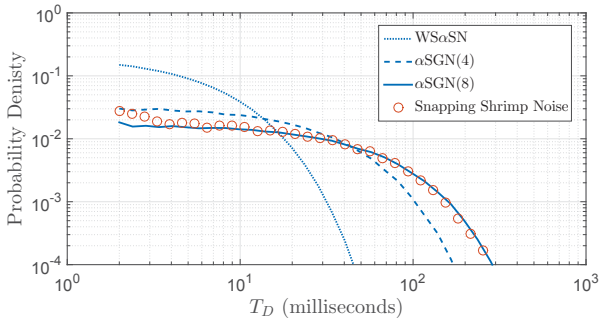

Fig. 13. PDFs of first-order inter-event intervals with dead-time filtering and threshold $30\hat{\delta}$ on a log-log scale.

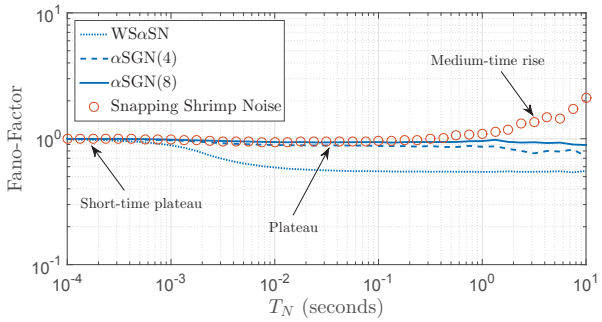

Fig. 14. Fano-factor against block length with dead-time filtering and threshold $30\hat{\delta}$.

events, which results in larger T_D and thus increased gradients with respect to Fig. 9. We plot the corresponding II results on the log and log-log scales in Figs. 12 & 13, respectively. As expected, the gradients of all curves in Fig. 12 are relatively increased. Moreover, the αSGN(8) curve still tracks that of the snapping shrimp data set very well. The corresponding FF curves are presented in Fig. 14 and offer similar trends to those in Fig. 11 but with slightly scaled down FFs.

V. Conclusion

We investigated the temporal characteristics of αSGN(m) for various m. This was accomplished by first tuning the model's parameters to practical snapping shrimp data. Noise realizations were then generated and converted to a point process in time via a threshold detector. The resulting time-series was investigated by employing first-order II arrival and FF analysis on raw and dead-time filtered data. These were then compared to results generated from the original snapping shrimp dataset. The pros and cons of modeling the latter with αSGN(m) was commented on. Overall, αSGN(m) was found to characterize the temporal statistics of snapping shrimp noise very well. Moreover, II analysis was found to be an effective tool in evaluating the order m of the model. This is necessary for characterizing snapping shrimp noise adequately.

References

[1] R. J. Urick, *Ambient Noise in the Sea*. Undersea Warfare Technology Office, Naval Sea Systems Command, Department of the Navy, Washington, D.C. 20362, 1984.

[2] W. W. L. Au and K. Banks, "The acoustics of the snapping shrimp synalpheus parneomeris in kaneohe bay," *The J. of the Acoustical Soc. of Amer.*, vol. 103, no. 1, pp. 41–47, 1998.

[3] M. W. Legg, "Non-gaussian and non-homogeneous poisson models of snapping shrimp noise," Ph.D. dissertation, Curtin Univ. of Technology, 2009.

[4] J. R. Potter, T. W. Lim, and M. A. Chitre, "Ambient noise environments in shallow tropical seas and the implications for acoustic sensing," *Oceanology Int.*, vol. 97, pp. 2114–2117, 1997.

[5] M. Chitre, J. Potter, and S.-H. Ong, "Optimal and near-optimal signal detection in snapping shrimp dominated ambient noise," *IEEE J. Ocean. Eng.*, vol. 31, no. 2, pp. 497 –503, April 2006.

[6] M. Chitre, J. Potter, and O. S. Heng, "Underwater acoustic channel characterisation for medium-range shallow water communications," in *OCEANS '04. MTTS/IEEE TECHNO-OCEAN '04*, vol. 1, Nov. 2004, pp. 40 –45.

[7] A. Mahmood, "Digital communications in additive white symmetric alpha-stable noise," Ph.D. dissertation, Natl. Univ. of Singapore, June 2014.

[8] M. Legg, A. Zaknich, A. Duncan, and M. Greening, "Analysis of impulsive biological noise due to snapping shrimp as a point process in time," in *OCEANS 2007 - Europe*, 2007, pp. 1–6.

[9] A. Mahmood and M. Chitre, "Modeling colored impulsive noise by markov chains and alpha-stable processes," in *Oceans - Genoa, 2015*, May 2015, pp. 1–7.

[10] K. Pelekanakis and M. Chitre, "New sparse adaptive algorithms based on the natural gradient and the L_0-norm," *IEEE J. Ocean. Eng.*, vol. 38, no. 2, pp. 323–332, April 2013.

[11] A. Mahmood, M. Chitre, and M. A. Armand, "Improving PSK performance in snapping shrimp noise with rotated constellations," in *Proc. of the Seventh ACM Int. Conf. on Underwater Networks and Systems*, ser. WUWNet '12, no. 12, New York, NY, USA, 2012, pp. 1–8.

[12] J. P. Nolan, "Multivariate elliptically contoured stable distributions: theory and estimation," *Computational Stat.*, vol. 28, no. 5, pp. 2067–2089, 2013.

[13] C. L. Nikias and M. Shao, *Signal processing with Alpha-Stable Distributions and Applications*. New York: Chapman-Hall, 1996.

[14] J. P. Nolan, *Stable Distributions - Models for Heavy Tailed Data*. Boston: Birkhauser, 2015, in progress, Chapter 1 online at. [Online]. Available: http://fs2.american.edu/jpnolan/www/stable/stable.html

[15] G. Samorodnitsky and M. S. Taqqu, *Stable Non-Gaussian Random Processes: Stochastic Models with Infinite Variance*. Chapman & Hall, 1994.

[16] A. Papoulis and U. S. Pillai, *Probability, Random Variables and Stochastic Processes*. Boston: McGraw-Hill, Dec 2001.

[17] M. Chitre, M. Legg, and T.-B. Koay, *Snapping shrimp dominated natural soundscape in Singapore waters*, ser. Contributions to Marine Sci. Nat. Univ. of Singapore, 2012.

[18] S. Kring, S. Rachev, M. Hchsttter, and F. Fabozzi, "Estimation of α-stable sub-gaussian distributions for asset returns," in *Risk Assessment*, ser. Contributions to Econ. Physica-Verlag HD, 2009, pp. 111–152.